

Analysis of the Effects of Vagal Stimulation on the Sinus Venosus of the Toad

F. R. Edwards, Narelle J. Bramich and G. D. S. Hirst

Phil. Trans. R. Soc. Lond. B 1993 **341**, 149-162
doi: 10.1098/rstb.1993.0099

Email alerting service

Receive free email alerts when new articles cite this article - sign up in the box at the top right-hand corner of the article or click [here](#)

To subscribe to *Phil. Trans. R. Soc. Lond. B* go to: <http://rstb.royalsocietypublishing.org/subscriptions>

Analysis of the effects of vagal stimulation on the sinus venosus of the toad

F. R. EDWARDS, NARELLE J. BRAMICH AND G. D. S. HIRST

Department of Zoology, University of Melbourne, Parkville, Victoria 3052, Australia

SUMMARY

In amphibians and mammals, vagal stimulation leads to the release of acetylcholine, ACh, which causes bradycardia. However, the responses to nerve stimulation are not well mimicked by exogenously applied ACh. These observations have led to the suggestion that there are subpopulations of muscarinic receptors on pacemaker cells and that during vagal stimulation neuronally released ACh caused slowing by suppressing inward current flow during diastole. After the generation of action potentials has been prevented by applying an organic calcium antagonist, vagal stimulation causes a hyperpolarization and an increase in membrane resistance: this observation suggests that the hyperpolarization results from a suppression of inward, presumably Na^+ , current flow.

In this study we describe the effects of vagal stimulation on membrane potentials recorded from arrested and beating hearts by using a computer model. The model of Noble & Noble (*Proc. R. Soc. Lond. B* **222**, 295 (1984)) was modified to describe the shape of amphibian pacemaker action potentials. A voltage-dependent Na conductance was included as well as two voltage-independent conductances, a background Na conductance and a background K conductance. Subsequently the hypothesis that the changes in membrane potential recorded during vagal stimulation from arrested preparations resulted from a reduction in Na conductance and this represented the sole action of vagally released ACh, was tested. If this were so, the changes in membrane conductance that occur during vagal inhibitory junction potentials recorded from arrested preparations should produce changes in pacemaker action potentials similar to those recorded experimentally from beating preparations. This was found to be the case. Thus the analyses are consistent with the idea that vagal inhibition of pacemaker cells results solely from a suppression of the two pacemaker sodium currents.

1. INTRODUCTION

In both amphibians and mammals, vagal stimulation leads to the release of acetylcholine, ACh, which causes bradycardia. When recordings were made from cardiac pacemaker cells, a characteristic sequence of membrane potential changes was observed. Trains of low frequency vagal stimuli increased the peak diastolic potential and reduced the rate of diastolic depolarization but had little effect on the amplitudes of pacemaker action potentials (Bywater *et al.* 1989; Campbell *et al.* 1989). Similar membrane potential changes were recorded following brief trains of high-frequency stimuli (Hutter & Trautwein 1955, 1956; Toda & West 1966; Shibata *et al.* 1985). With long trains of high frequency stimuli, the generation of pacemaker action potentials stopped and the membrane potential settled at a value positive of the peak diastolic potential (Bywater *et al.* 1989; Campbell *et al.* 1989). From these observations it was suggested that during vagal stimulation neuronally released ACh suppressed inward current flow during diastole and slowed the rate of diastolic depolarization (Bywater *et al.* 1989; Campbell *et al.* 1989). Cessation of beating would then occur when the inward current during

diastole was insufficient to drive the membrane potential to threshold for the initiation of an action potential. Although the effects of vagal stimulation were readily abolished by the muscarinic antagonist hyoscine, the responses were not readily mimicked by bath-applied ACh (Bywater *et al.* 1989; Campbell *et al.* 1989). Applied ACh also slowed the rate of discharge of pacemaker cells by activating a muscarinic receptor but this was associated with a large increase in peak diastolic potential and a shortening of the duration of action potentials. When a concentration of ACh, sufficient to stop beating, was applied the membrane potential settled to a value negative of the peak diastolic potential. Presumably ACh, applied in this way, activates a different subset of muscarinic receptors which leads to an increase in potassium conductance.

In amphibians and mammals, after the generation of action potentials has been prevented by applying a calcium antagonist, vagal stimulation causes membrane hyperpolarization (Hartzell 1979; Jalife & Moe 1979; Bywater *et al.* 1989, 1990; see also Del Castillo & Katz 1955). In these preparations, the voltage-dependent channels involved in pacemaking activity essentially are inactivated. Although similar membrane

potential changes to those produced by vagal stimulation were produced by the applied ACh, the responses could be differentiated by adding barium ions, Ba^{2+} , to the physiological saline. With Ba^{2+} present, the responses to applied ACh were much reduced but those to vagal stimulation persisted. Furthermore, the membrane resistance of arrested sinus venosus preparations increased during a vagal hyperpolarization and fell during the application of ACh (Bywater *et al.* 1990). Clearly the increase in membrane resistance during vagal stimulation could have been a consequence of the hyperpolarization itself. Alternatively, the hyperpolarization and increased membrane resistance may both result from a suppression of inward, presumably Na^+ , current flow.

In this study we set out to see if the effects of vagal stimulation on membrane potentials recorded from arrested and beating hearts could be described by using a computer model. As a starting point the model describing the sino-atrial node, formulated by Noble & Noble (1984) and DiFrancesco & Noble (1985), was used to describe the shape of amphibian pacemaker action potentials. Appropriate modifications were made to allow an adequate description of amphibian pacemaking activity. We subsequently made the assumption that the changes in membrane potential recorded during vagal stimulation from arrested preparations represented the sole action of vagally released ACh. If this were the case, the changes in membrane conductance that occur during vagal inhibitory junction potentials recorded from arrested preparations (see Bywater *et al.* 1990) should produce changes in pacemaker action potentials similar to those recorded experimentally from beating preparations (see Bywater *et al.* 1989). With this approach the analyses are consistent with the idea that vagal inhibition of pacemaker cells results solely from a suppression of pacemaker sodium currents.

2. METHODS

(a) Collection of physiological data

Intracellular recordings were made from preparations of sinus venosus of toads, *Bufo marinus*. Toads were anaesthetized by using an aqueous solution of 0.5% tricaine methanesulfonate. Preparations, consisting of the sinus venosus in continuity with the two atria, with attached left and right vago-sympathetic trunks, dissected back to the intracranial vagal roots, were pinned out in a shallow recording chamber. Vagal fibres alone were stimulated by drawing the two intracranial roots, some 3 mm central to the vagal ganglion, between a pair of stimulating electrodes (stimulation voltages 3–10 V, pulse width 1.0 ms). The selectivity of vagal stimulation was checked by using the muscarinic antagonists atropine, hyoscine

stimulation, suggesting that muscarinic receptors were being activated and that the vagal pathway was interrupted by a ganglionic synapse. The preparations were continuously perfused at a rate of 6 ml min^{-1} (bath volume 1 ml) with a physiological saline (composition in millimoles per litre: NaCl, 115; KCl, 3.2; $NaHCO_3$, 20; NaH_2PO_4 , 3.1; $CaCl_2$, 1.8; $MgCl_2$, 1.4; glucose, 16.7; gassed with 95% oxygen: 5% carbon dioxide); all experiments were carried out at room temperature, 20–25°C. In some experiments nicardipine ($1 \times 10^{-5} \text{ M}$) was added to this solution to prevent the spontaneous generation of cardiac action potentials. In some experiments the external concentration of chloride ions was reduced by exchanging sodium chloride with sodium isethionate and in others with sodium methyl sulphate.

Membrane potentials were recorded from cells which lay in the exposed centre of the dorsal wall of the sinus venosus, some 5–7 mm distant from the sino-atrial aperture, using conventional techniques with fine glass micro-electrodes (resistances 80–150 M Ω , filled with 0.5 M KCl). Pacemaker cells were selected on the basis that the diastolic depolarization led smoothly into the upstroke of the pacemaker action potential. Recordings were taken from a number of muscle bundles until such recordings were obtained. All membrane potential records were low-pass filtered, cut-off frequency 1 kHz, digitized and stored on disk for later analysis. For further details see Bywater *et al.* (1989, 1990).

(b) Description of computer simulation of pacemaker action potentials

The generation of pacemaker action potentials, as recorded from the toad sinus venosus, was described by using the model provided by Noble & Noble (1984) for pacemaking activity in the mammalian sinoatrial node. The equations used to define the various membrane currents along with their voltage and time dependencies are given in DiFrancesco & Noble (1985). Where necessary, the equations were amended on the advice of Professor D. Noble; we express our gratitude. The nomenclature follows that of DiFrancesco & Noble (1985). More recent expressions to describe the gating of i_K and i_f given by Noble *et al.* (1989) were used. The equation used to describe $i_{K,ACh}$ is that given by Egan & Noble (1987).

(c) Description of variables specifically related to the toad sinus venosus preparation

The description of pacemaking activity is based on the assumption that the cells are closely coupled electrically so that the syncytium may be considered isopotential (see Bywater *et al.* 1990). The membrane potential, E_m , under isopotential conditions is given by

$$dE_m/dt = -(i_f + i_K + i_{K1} + i_{b,K} + i_{b,Na} + i_{b,Ca} + i_p + i_{NaCa} + i_{Na} + i_{Ca,t})/C_m, \quad (1)$$

and 4-DAMP and the nicotinic antagonist tubocurarine. Each of these agents in appropriate concentrations entirely abolished the response to vagal

where C_m is the membrane capacitance and the individual currents are designated as follows: i_f , the hyperpolarization-activated inward current; i_K ,

the delayed rectifier K current; i_{K1} , the inward rectifier current; $i_{b,K}$, the voltage- and time-independent background K current; $i_{b,Na}$, the voltage- and time-independent background Na current; $i_{b,Ca}$, the voltage- and time-independent background Ca current; i_p , the Na/K exchange pump current; i_{NaCa} , the Na/Ca exchange current; i_{Na} , the voltage-dependent Na current; $i_{Ca,f}$, the voltage-dependent Ca current.

(i) *Principal currents present in the arrested heart, $i_{b,K}$, $i_{b,Na}$, i_p*

After preventing the generation of action potentials with an organic calcium antagonist, sinus venosus cells have stable membrane potentials of -35 mV, their membrane time constants are about 500 ms (Bywater *et al.* 1990). Furthermore, the membrane potential is unchanged by the addition of agents which block i_K , i_{K1} , i_f and i_{Na} . If it is assumed that the principal ion pathways across the membrane consist of background

$$a_d = 30(E_m + 49)/\{1 - \exp[-(E_m + 49)/0.4]\} \quad \text{cf. equation 41} \quad (5)$$

$$(a_d)_{E_m = -49} = 120 \quad \text{cf. equation 41a} \quad (6)$$

$$b_d = 12(E_m + 49)/[\exp(E_m + 49) - 1] \quad \text{cf. equation 42} \quad (7)$$

$$(b_d)_{E_m = -49} = 120 \quad \text{cf. equation 42a} \quad (8)$$

$$a_f = 2.08(E_m + 59)/\{\exp[(E_m + 59)/1.33] - 1\} \quad \text{cf. equation 44} \quad (9)$$

$$(a_f)_{E_m = -59} = 8.33 \quad \text{cf. equation 44a} \quad (10)$$

$$b_f = 16.67/\{1 + \exp[-(E_m + 49)/1.33]\} \quad \text{cf. equation 45} \quad (11)$$

(all in DiFrancesco & Noble 1985).

ohmic K channels and Na channels together with a Na/K exchange pump, values for $g_{b,Na}$ of $0.082 \mu\text{S}$ (equation (19), DiFrancesco & Noble 1985), for $g_{b,K}$ of $0.114 \mu\text{S}$ (see equation (60), DiFrancesco & Noble 1985) and for \bar{i}_p of 29 nA (equation (21), DiFrancesco & Noble 1985) simulate the experiment observations and maintain the specified intracellular ionic conditions (see Initial Conditions). The value for background K current is given by

$$i_{b,K} = g_{b,K} (E_m - E_K), \quad (2)$$

where E_K is the potassium equilibrium potential.

(ii) *Characterization of hyperpolarization activated inward current, i_f :*

Stimulation of the vagus hyperpolarizes the membranes of arrested sinus preparations. The hyperpolarization resulting from intense vagal stimulation, after a delay, appears to activate i_f leading to some recovery of membrane potential during continued stimulation. (figure 6*b*). This view is based on the finding that recovery is blocked by adding Cs^+ to the physiological saline (figure 7*b*). Our estimates of the magnitude and temporal characteristics of i_f are based on the difference between vagal responses recorded in the presence and absence of Cs^+ . Peak values of $g_{f,K}$ and $g_{f,Na}$ were set to $600 \mu\text{S}$ (equation 3, DiFrancesco & Noble 1985). The rate coefficients of gating variable y , used to describe kinetics of opening and closing of i_f , were set to

$$a_y = 0.002 \exp(-E_m/27) \quad (3)$$

cf. equation 9 (Noble *et al.* 1989)

$$b_y = 1.95 \exp(E_m/28.5) \quad (4)$$

cf. equation 10 (Noble *et al.* 1989).

Compared with the mammalian model, the kinetics were slowed by a factor of 10 and the voltage sensitivity of the activation process was reduced.

(iii) *Description of inward currents, $i_{Ca,f}$ and i_{NaCa}*

In the toad, the addition of TTX to a beating sinus venosus slows the rate of generation of action potentials presumably by blocking i_{Na} channels (figure 2). The slowed action potential then results from the activation of $i_{Ca,f}$, i_{NaCa} , i_f and i_K acting upon a composite of the currents present during arrest.

To fit data, the permeability factor, P_{si} , for $i_{Ca,f}$ was set at 30 nA mm^{-1} (equation 38 and 39, DiFrancesco & Noble 1985) and the voltage dependencies of the activation and inactivation processes were modified as shown in the following equations:

These modifications result in $i_{Ca,f}$ having a threshold for activation 25 mV more negative than the mammalian model, primary inactivation slowed by a factor of 3 and increased voltage sensitivity of the activation and inactivation processes.

The Na/Ca exchange current was computed using equation 26 (DiFrancesco & Noble 1985) and the scaling factor, k_{NaCa} , was made 0.1.

(iv) *Treatment of delayed rectifier current, i_K*

The delayed rectifier scaling value, $i_{K,max}$, was made 91 (equation 8, DiFrancesco & Noble 1985). The voltage dependencies of the activation and deactivation processes (equations 4 and 5, Noble *et al.* 1989) were modified by changing the coefficients from 2.1 to 0.55 and 0.96 to 0.17, respectively. The activation of i_K proceeds about four times more slowly than the mammalian model and deactivation about six times more slowly.

(v) *Contribution of a voltage-dependent sodium current, i_{Na}*

Although a voltage-dependent sodium current is generally thought to be absent during pacemaking activity, in the toad TTX, 1×10^{-6} M, consistently slows the rate of generation of pacemaker action potentials. This finding is dealt with in detail in the Results section. On the assumption that this effect of TTX results from its ability to block voltage-dependent Na channels, a current i_{Na} , has been included in the simulations. The fast sodium conductance g_{Na} was set to $50 \mu\text{S}$ (equation 28, DiFrancesco & Noble 1985). The kinetics of the inactivation process were slowed by a factor of 4, hence in equation 35

(DiFrancesco & Noble 1985) the coefficient 20 becomes 5 and in equation 36 (DiFrancesco & Noble 1985) the coefficient 2000 becomes 500. In the expression for β_m (equation 34, DiFrancesco & Noble 1985) the coefficient -0.056 was replaced with -0.112 . The rate of decay of activation is then more dependent upon membrane voltage.

(vi) *Estimates of $i_{b,Ca}$, i_{K1}*

The resting Ca^{2+} leak conductance $g_{b,Ca}$ was chosen as $0.001 \mu S$ (equation 27, DiFrancesco & Noble 1985) to compensate the small outward Ca^{2+} component of i_{NaCa} present in the arrested model. As Ba^{2+} had little effect on beating and arrested membrane potentials, the inwardly rectifying K^+ conductance g_{K1} was assumed to be very small and set at $10 \mu S$ (equation 13, DiFrancesco & Noble 1985).

For simulations of bath application of ACh the current $i_{K,ACh}$ was added to the membrane current sum

(vii) *Membrane capacitance and intracellular volume*

In our description the syncytium had a total membrane capacitance of $0.1 \mu F$. For comparison Rasmusson *et al.* (1990), in their description of pacemaking activity in a single bullfrog sinus cell, use a value of $75 pF$ for the nominal capacitance; a capacitance of $0.1 \mu F$ is then equivalent to 1330 cells. The value used for the intracellular volume of the syncytium, $0.0032 \mu l$, was based on an assumption of cylindrical cell shape. Giles & Shibata (1985) describe the bullfrog sinus cell as being spindle shaped with a maximum diameter of $5-7 \mu m$ at the nucleus and a length of $250-300 \mu m$. This implies a preparation having an intracellular volume of $0.0039 \mu l$: a volume change of this size makes little difference to the computations.

(viii) *Initial conditions*

The following initial conditions were used for simulations of normally beating tissue.

$$E_m = -67.4 \text{ mV,}$$

$$[Ca]_i = 2 \times 10^{-5} \text{ mM,}$$

$$[Ca]_{rel} = 0.0295 \text{ mM,}$$

$$[Ca]_{up} = 0.0296 \text{ mM,}$$

$$[Ca]_o = 1.8 \text{ mM,}$$

$$[Na]_i = 7.5 \text{ mM,}$$

$$[Na]_o = 140 \text{ mM,}$$

$$[K]_i = 140 \text{ mM,}$$

$$[K]_e = 3.46 \text{ mM,}$$

$$[K]_b = 3.0 \text{ mM,}$$

$$y = 0.0157, i_f \text{ gating variable}$$

$$m = 0.0323, i_{Na} \text{ activation gating variable}$$

$$h = 0.321, i_{Na} \text{ inactivation gating variable}$$

$$d = 7 \times 10^{-22}, i_{Ca,f} \text{ activation gating variable}$$

$$f = 0.993, i_{Ca,f} \text{ inactivation gating variable}$$

$$f_2 = 0.98, i_{Ca,f} \text{ Ca}^{2+} \text{-dependent inactivation}$$

$$x = 0.126, i_K \text{ gating variable}$$

$$p = 0.795 \text{ internal Ca store exchange variable.}$$

(ix) *Conductance modulations*

Conductance modulations representing the responses to applied pharmacological agents or to vagal stimulation were simulated with sigmoidal onset and offset functions each having specified half-peak time and gradient.

(d) *Computational methods*

The SCoP (version 2.61) modelling package (Simulation Resources, Inc, Durham, NC, NIH grant RR01693) was used for all simulations and optimizations. The integrating algorithms were provided by the Livermore Solver for Ordinary Differential Equations, a subroutine package which is suited to solving sets of equations whose dominant time constants are dissimilar. Different integrating algorithms and suitable step sizes were selected automatically depending on the gradients of the variables under solution. SCoP was configured to run under MS-DOS 3.30 on a desktop computer. On a 33MHz 80386 computer with coprocessor the computations for a beating sinus proceed about 10 times slower than real time.

3. RESULTS

(a) *Pacemaker potentials in sinus venosus of toads*

When intracellular recordings were made from toad sinus venosus cells, regular discharges of pacemaker action potentials were recorded. These potentials had similar shapes and amplitudes to those recorded from pacemaker cells of other amphibians and mammals (see Noble 1975). Action potentials had maximum diastolic potentials in the range -60 mV to -78 mV (mean $-70.5 \pm 1.3 \text{ mV}$; $n = 12$) and occurred at 33–50 beats per minute (mean 41.8 ± 0.3 beats per minute; $n = 12$). Each slow diastolic depolarization led smoothly into an action potential, the rapid upstroke of the action potentials being initiated at a threshold potential of about -50 mV . The rising phases of action potentials recorded from pacemaker cells were briefer, $\approx 50 \text{ ms}$, than the repolarization phases, $\approx 400 \text{ ms}$. Pacemaker action potentials had amplitudes, when measured from the maximum diastolic potential to the peak of the action potential, of about 110 mV (mean $107.3 \pm 3.4 \text{ mV}$; $n = 12$): hence each pacemaker action potential overshoot the zero potential by about 30 mV . As has been pointed out previously, pacemaker action potentials recorded from these preparations have large amplitudes if high-resistance microelectrodes are used (see Bramich *et al.* 1990). These action potentials had slow rates of rise with a mean dV/dt_{max} of $8.7 \pm 0.9 \text{ V s}^{-1}$.

During each pacemaker action potential a set of voltage-dependent Ca channels open to provide an inward current carried by Ca^{2+} (Noble 1975). Recently it has been shown that in mammals Ca channels may be subdivided into two types, Ca_T and Ca_L channels (Hagiwara *et al.* 1988). Ca_T channels open at quite negative membrane potentials and in rabbit sino-atrial node cells transiently supply an

inward Ca^{2+} current during the diastolic depolarization: Ca_T channels are blocked by nickel ions (Hagiwara *et al.* 1988). Ca_L channels open at more positive membrane potentials than do Ca_T channels and supply a longer-lasting inward Ca^{2+} current: these channels are blocked by organic Ca antagonists such as nifedipine or nifedipine (Hagiwara *et al.* 1988). In toad preparations (four preparations) the rate of generation of pacemaker action potentials was unchanged when nickel ions, 1 mM, were added to the physiological saline. Hence in the simulations of pacemaker actions it has been assumed that Ca_T channels are absent from toad sinus venosus cells. Pacemaker action potentials were, however, abolished by adding nicardipine (1×10^{-5} M) or nifedipine (1×10^{-5} M) to the physiological saline. Therefore we have used the general description for the total inward Ca^{2+} current, referred to as $i_{\text{Ca},f}$ provided by DiFrancesco & Noble (1985). To fit data it was necessary to set the activation potential for $i_{\text{Ca},f}$ at a value some 25 mV more negative than that suggested by DiFrancesco & Noble (1985) for mammalian cardiac tissues; as such the threshold agrees well with that determined experimentally in amphibian pacemaker cells (Rasmusson *et al.* 1990).

As the membrane depolarizes, a set of delayed rectifier K channels opens and provides an outward K^+ current, i_K , which returns the membrane potential to negative values. For pacemaking to occur, i_K must show time- and voltage-dependent deactivation. For the purposes of this analysis we have adopted the general description of this current provided by Noble *et al.* (1989).

The sources of the inward current flowing during diastole are controversial. In our view, in the toad, inward current during diastole is provided by at least three distinct sets of channels or membrane conductances. Firstly an inward current flows through a voltage-independent background sodium conductance, $g_{b,\text{Na}}$; this current is likely to be partly offset by outward current flow through a voltage-independent background potassium conductance, $g_{b,\text{K}}$ (see equation 60, Noble & DiFrancesco 1985). A second inward current is provided by a set of voltage-dependent Na channels which are blocked by tetrodotoxin (TTX). The third current is provided by a set of voltage-dependent hyperpolarization activated Na/K channels. These channels are activated at membrane potentials negative of about -40 mV; they allow the influx of Na^+ and the efflux of K^+ : these channels are blocked by caesium ions (Cs^+). These currents, flowing through separate channels, will be discussed in turn, along with the justification for their inclusion as having a role in pacemaking activity in toad sinus venosus cells.

When pacemaker action potentials were abolished by adding either nifedipine or nicardipine, 1×10^{-5} M, the membrane potential settled at a potential of about -35 mV (-33.2 ± 0.7 mV; $n=12$). An experimental observation is shown in figure 1*a*. A pacemaker action potential was recorded in control solution and the steady potential was recorded some 60 min after adding nicardipine to the physiological saline. To

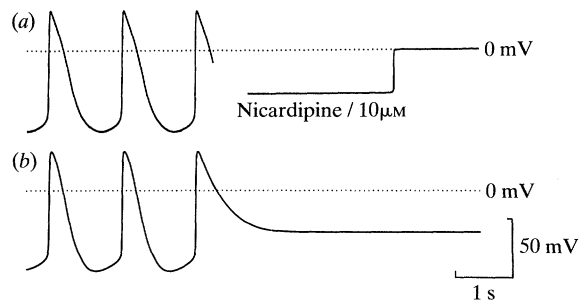


Figure 1. The effect of blocking calcium channels on the generation of pacemaker action potentials recorded from toad sinus venosus muscle. (a) The traces were recorded firstly in control solution and subsequently from the same preparation, 1 h after adding nicardipine, 1×10^{-5} M, to the physiological saline. It can be seen that in control solution a rhythmic discharge of action potentials was recorded. After abolition of pacemaking activity the membrane potential was stable and had a value of about -35 mV; at the end of this trace the electrode was withdrawn to check the zero potential. (b) A simulation of pacemaking activity. After three action potentials both the voltage-dependent calcium channels and the delayed rectifier K channels were closed. The conductances of $g_{b,\text{Na}}$, $g_{b,\text{K}}$ and i_p had been adjusted so that in the simulation the membrane potential settled at a value similar to that recorded experimentally. The time and voltage calibration bars refer to both sets of recordings.

determine if any of the conventional voltage-dependent channels which have been shown to be present in cardiac tissues made major contributions to the stable potential, the effects of a number of channel blocking agents on arrested preparations were examined. In each of six experiments, adding barium ions (Ba^{2+} , 1 mM) to the physiological saline produced no detectable change in membrane potential. This suggests that inward rectifier K channels, which are blocked by Ba^{2+} (Hille 1984), make little contribution to the arrested membrane potential: this is perhaps not surprising as these channels have been shown to be absent from pacemaker cells in other species (Shibata & Giles 1985). A contribution made by hyperpolarization-activated Na/K channels could not be detected experimentally; Cs^+ (5 mM on six preparations and 2 mM on three preparations), added to the physiological saline failed to produce a detectable membrane potential change. This observation does not imply that these channels are absent from toad sinus pacemaker cells (see figure 4), rather it suggests that these channels are closed at -35 mV. TTX (1×10^{-6} M; four preparations) produced a small and variable hyperpolarization, range 1–3 mV. Delayed rectifier K channels did not appear to contribute to the arrested potential; the addition of tetra-ethylammonium ions (10 mM; three preparations), which block delayed rectifier K channels (Denyer & Brown 1990), failed to produce a detectable change in the membrane potential of arrested preparations.

Hence we suggest that the stable membrane potential recorded from these arrested preparations results predominantly from the balance between a background sodium conductance $g_{b,\text{Na}}$ and an analogous background conductance, $g_{b,\text{K}}$ (see also DiFrancesco

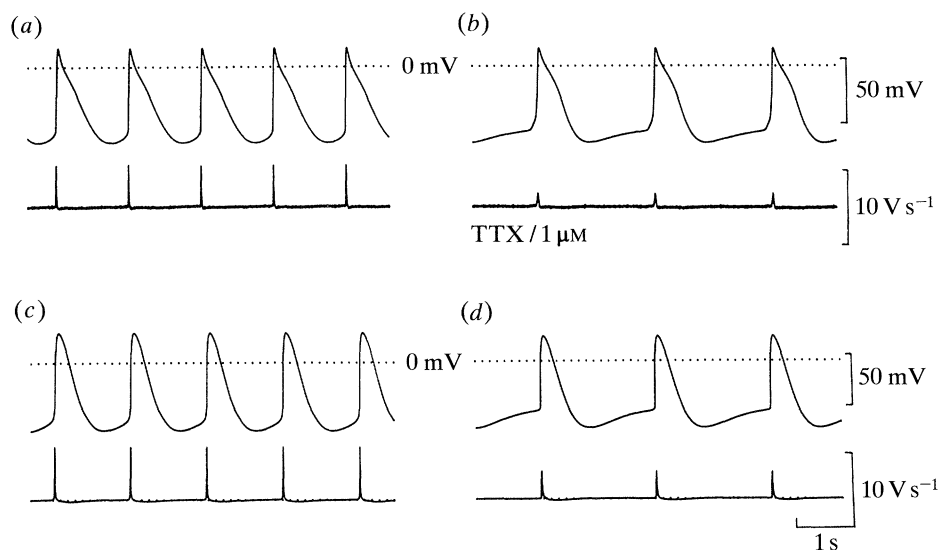


Figure 2. Effect of TTX on the discharge of pacemaker action potentials recorded from a toad sinus venosus cell. (a) Along with an associated dV/dt trace, this shows a recording from a pacemaker cell obtained in control solution; (b) with associated dV/dt trace, this shows a recording from the same cell 5 min after adding TTX, 1×10^{-6} M, to the physiological saline. It can be seen that the rate of discharge of action potentials has fallen by about one third, the rate of diastolic depolarization is reduced and dV/dt_{\max} has fallen from 5.6 V s^{-1} to 1.7 V s^{-1} . (c) and (d) show the computer simulations that were derived to describe the effect of TTX. In (c) a series of control action potentials are presented. A part of the inward current during diastole is provided by a set of voltage-dependent Na channels. The properties of these channels were adjusted so that (d) when they were blocked the simulation had a form much like that of the action potential recorded experimentally, as illustrated in (b). The time calibration bar refers to all records.

& Noble 1985). A contribution to the arrested potential is also made by an electrogenic sodium pump (DiFrancesco & Noble 1985). When the passive membrane properties of arrested sinus preparations were determined, the membrane time constant was found to be ≈ 500 ms: assuming that specific membrane capacitance is $1 \mu\text{F} \cdot \text{cm}^{-2}$ the specific membrane resistance must be about $500 \text{ k}\Omega \text{ cm}^2$ (see Bywater *et al.* 1990). Thus if one assumes that E_{Na} and E_{K} are $+40$ mV and -90 mV, respectively, the absolute levels of the two background conductances can be set so that the arrested potential is the same as that determined experimentally (-35 mV). With this approach the ratio of $g_{\text{b,K}}$ to $g_{\text{b,Na}}$ was 15:11. The specific background sodium conductance was $0.82 \mu\text{S cm}^{-2}$ and the specific background potassium conductance was $1.14 \mu\text{S cm}^{-2}$. Clearly, unless $g_{\text{b,Na}}$ is present only in arrested preparations, it will provide an inward current throughout the pacemaker cycle. The amplitude of the current at any instant will be determined by the difference between the membrane potential and E_{Na} (see Noble 1984) with the current being maximal during diastole. Similarly the outward current through $g_{\text{b,K}}$ will be minimal during diastole.

For mathematical purposes the description of the arrested membrane potential contains a contribution provided by an an electrogenic Na/K exchange mechanism, along with small contributions from a background calcium conductance, a Na/Ca exchange mechanism, voltage-dependent Na channels, i_{Na} , and hyperpolarization-activated Na/K channels, i_{f} . As would be expected in a simulation of pacemaking

activity, when both voltage-dependent Ca channels and delayed rectifier K channels were inactivated, the membrane potential is dominated by $g_{\text{b,Na}}$ and $g_{\text{b,K}}$ and settles at -35 mV (figure 1b).

A second inward current, i_{Na} , which was included in the description of pacemaking activity, was provided by a set of voltage-dependent Na channels. Such channels are usually considered either to be absent from pacemaker tissues (Giles & Shibata 1985) or only re-activated when the membrane potential is made very negative (Kreitner 1975). However, more recent studies have suggested that these channels may be active during pacemaking activity in mammalian sinoatrial node cells (Denyer & Brown 1990). In the sinus venosus of the toad TTX invariably reduces the rate of generation of pacemaker action potentials (Bywater *et al.* 1989). In this series of experiments the rate of generation of pacemaker action potentials fell to about 50% of the control rate within 5 min of adding TTX, 1×10^{-6} M, to the physiological saline (mean rate in control solution, 42 ± 4 beats per minute; mean rate in TTX-containing solution, 21 ± 3 beats per minute; $n=5$; figure 2a,b). Much of the change in form of the membrane potential recordings occurred during the diastolic interval. The form of this 'pacemaking' Na^+ current was described by using the equations given by DiFrancesco & Noble (1985) with the intensity of conductance modulation, the activation potential and the time constants of activation and inactivation being adjusted until a good fit with control and TTX-treated data was obtained (figure 2c,d).

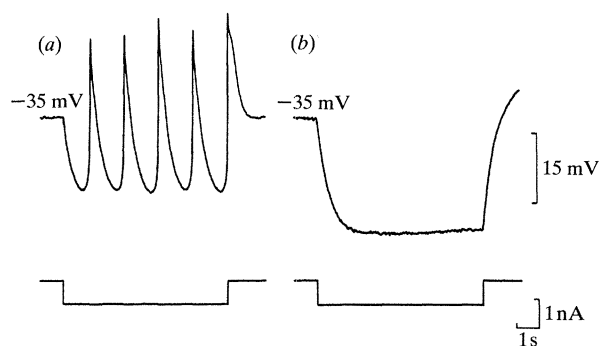


Figure 3. The effect of TTX on the discharge of regenerative potentials recorded from a small segment of sinus venosus muscle. The segment was impaled with two electrodes, one to record membrane potential and one to pass current. Throughout, the physiological saline contained, nicardipine, 1×10^{-5} M, Cs^+ , 5 mM, and Ba^{2+} , 1 mM. The upper pair of the traces shown in (a) shows the membrane potential change caused by passing a hyperpolarizing current, intensity shown in lower trace, through the current passing electrode. It can be seen that as the membrane was hyperpolarized, a series of regenerative potential changes were detected. The traces in (b) show a recording from the same preparation 5 min after the further addition of TTX, 1×10^{-6} M. It can be seen that now the same hyperpolarizing current produces only an electrotonic potential that is not interrupted by regenerative membrane potential changes. Voltage calibration bar refers to upper records; current calibration bar refers to lower records. Time calibration bar refers to all records.

We were concerned that, because our experiments were carried out on the intact sinus venosus along with surrounding atrial muscle, the voltage records could be 'contaminated' by Na currents from non-pacemaker tissues. In a separate series of experiments, small segments of tissue were taken from the central region of the sinus venosus. These preparations were cut along the axial direction of muscle bundles to have lengths of some 200–300 μm and widths of 40 μm . As such they would be expected to be isopotential (see Bywater *et al.* 1990). The preparations were impaled with two microelectrodes and were bathed in physiological saline which contained nicardipine, 1×10^{-5} M, and Ba^{2+} 1 mM. The preparations had stable membrane potentials in the range -27 mV to -35 mV. When hyperpolarizing current pulses were passed through one electrode so that electrotonic potentials with amplitudes of less than 5 mV were recorded, their timecourses could be described by single exponentials with time constants in the range 290–530 ms (mean 370 ± 20 ms; $n=11$). These values are very similar to those calculated for the intact tissue assuming it to be a two-dimensional syncytium (Bywater *et al.* 1990). When the membrane potential was hyperpolarized to lie in the range -50 mV to -90 mV, the electrotonic potentials were not well sustained presumably due to the activation of hyperpolarization activated Na/K channels (see Brown 1982; DiFrancesco & Noble 1989). When Cs^+ , 5 mM, was added to the tissue fluid this relaxation due to i_f was blocked. Now when the membrane was hyperpolarized so the

potential lay in the range -50 mV to -65 mV, a series of rhythmical potential changes were recorded (figure 3a). These membrane potential changes were abolished by the subsequent addition of TTX, 1×10^{-6} M (figure 3b). As these oscillations were not detected until after the addition of Cs^+ , it must be assumed that normally the increase in conductance produced by hyperpolarization activated Na/K channels is sufficient to shunt out the current due to the presence of voltage-dependent Na channels. From these observations it seems that a set of voltage-dependent Na channels is present in some of the cells lying in centre of the sinus venosus. As the TTX-sensitive membrane potential oscillations were detected at potentials positive of -70 mV (see figure 3a), the Na channels responsible will be re-activated during the falling phase of the action potential and will contribute an inward current during the diastolic depolarization.

The third set of channels which give rise to inward current during pacemaking activity are hyperpolarization-activated Na/K channels (Yanagihara & Irisawa 1980; Brown 1982; DiFrancesco 1985). In five experiments the effect of Cs^+ on the rate of generation of action potentials was examined. The addition of Cs^+ , 5 mM, reduced the rate of generation of action potentials (mean rate in control solution 34 ± 2 beats per minute; rate in Cs^+ -containing solution 14 ± 2 beats per minute, figure 4a; see also Bywater *et al.* 1989). However, when the shapes of the action potentials were inspected it became apparent that only the initial 20% reduction in rate could be attributed to a change in the form of the membrane potential during the diastolic interval. That is, at the onset of application of a Cs^+ -containing solution, the rate of diastolic depolarization was slowed and the rate of generation of action potentials fell to 80% of the control rate. During prolonged exposure, although the rate of generation of action potentials continued to fall, the later stage of slowing did not appear to be associated with an effect on i_f , rather it was associated with a slowing in the rate of action potential repolarization. Similar effects were produced by lower concentrations of Cs^+ ; 1 mM Cs^+ slowed the heart rate by 27%, $n=3$; 2 mM Cs^+ slowed the heart rate by 54%, $n=4$. The slowing produced by 1 mM Cs^+ was associated solely with a reduced rate of diastolic depolarization, suggesting that the more pronounced slowing detected in 2 mM and 5 mM Cs^+ resulted from an action of Cs^+ on other membrane channels than those responsible for the generation of i_f . In the computations i_f was described using the equations given by Noble *et al.* (1989) with the conductance and time constant of activation being adjusted both to give a 20% reduction in rate (see figure 4a,b) and to fit data obtained from arrested preparations (see figures 6 and 7). To do this the rate constants were made slower than those described for mammalian cells (see Methods).

Having set the background Na^+ and K^+ conductances and i_f , the activation parameters of $i_{\text{Ca},f}$ and i_{K} were varied until good fits to experimental data recorded in TTX-containing solutions were obtained.

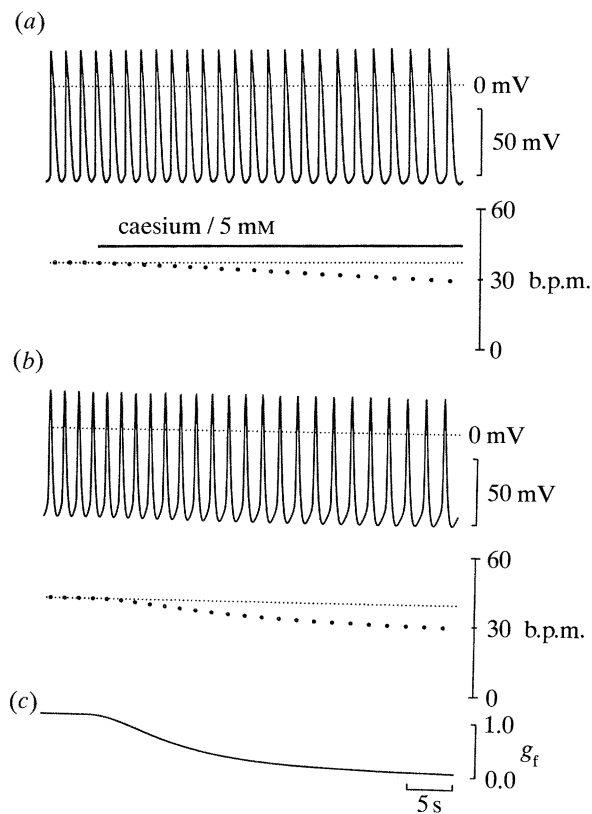


Figure 4. Effect of Cs^+ on the discharge of pacemaker action potentials recorded from a toad sinus venosus cell. Trace (a) shows a recording from a pacemaker cell obtained during the addition of Cs^+ , 5 mM, to the physiological saline. It can be seen that the rate of discharge of action potentials falls and this is associated with a slowed rate of diastolic depolarization and a slight increase in peak diastolic potential. Trace (b) shows the computer simulation that was derived to describe the effect of Cs^+ . It was assumed that slowing resulted from the ability of Cs^+ to block i_f . The properties of hyperpolarization activated Na/K channels were adjusted so that they fitted data obtained from the responses to vagal stimulation (see Methods along with figures 6 and 7). When i_f was inactivated, with the timecourse shown in (c), the simulation had a form much like that of the experiment record shown in (a). The conductance calibration bar represents the conductance modulation applied to g_f normalized about its control value.

The timecourses of control pacemaker action potentials were calculated by incorporating the description of i_{Na} derived above. The mathematical description of each current followed that derived by Noble & DiFrancesco (1985); the parameters used for descriptions of toad pacemaker cell action potentials are given in the Methods.

A set of experimental data (figure 5a) is compared with a calculation (figure 5b) along with the currents flowing during the simulation in figure 5. This description of pacemaking is in line with the view that a number of currents flow during diastole and pacemaking activity cannot be ascribed to any single current (Brown 1982; Noble 1984). In addition it will be appreciated that our approach differs from that often taken. The description of pacemaking activity presented here is based on the observed effects of

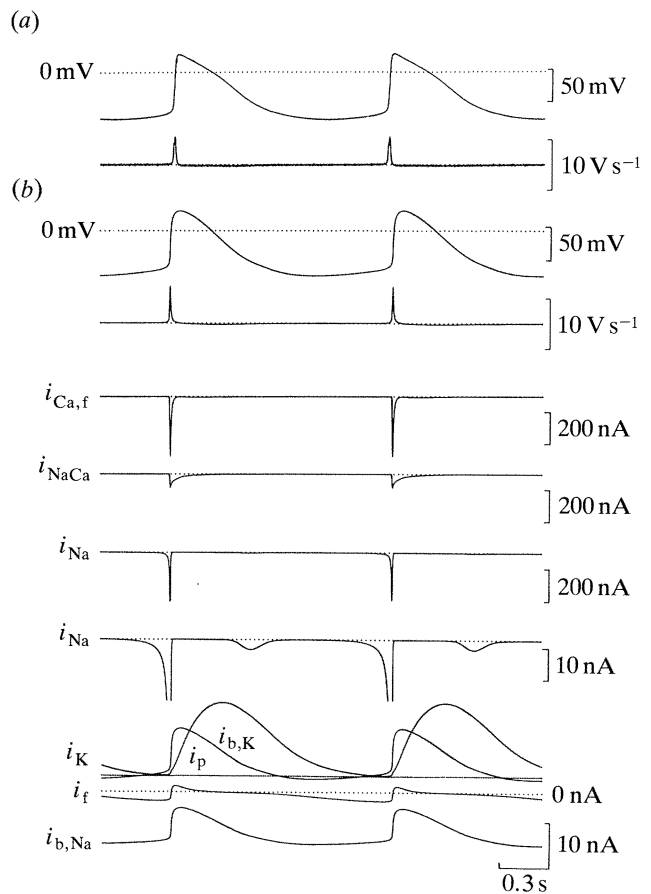


Figure 5. Summary of membrane currents flowing during pacemaking activity in sinus venosus of the toad. Trace (a) shows a membrane potential recording, along with its associated dV/dt trace, from a pacemaker cell in the toad sinus venosus. Trace (b) shows a computer simulation of pacemaking activity in this tissue followed by the various membrane currents flowing during the simulated pacemaker action potential. The first three current traces show the dominant inward currents flowing during the upstroke of the action potential; these are $i_{\text{Ca},f}$, i_{NaCa} and i_{Na} . The fourth current trace again shows i_{Na} but at increased gain; it is apparent that in the simulation there is an appreciable inward Na^+ current during the latter phases of diastole. The lower family of five current traces show the dominant currents flowing during diastole. It can be seen that the dominant outward currents are i_{K} and an outward current, $i_{\text{b},\text{K}}$, provided by a background potassium conductance. During the pacemaker cycle, there is little variation in the current, i_{p} , provided by an electrogenic Na/K transport system, shown as the dotted line. The other inward currents flowing during pacemaking activity are provided by i_{f} and a current, $i_{\text{b},\text{Na}}$, flowing through a background sodium conductance. It is apparent that the dominant inward current flow during diastole is provided by the background sodium conductance. The time calibration bar refers to all traces.

channel blocking-drugs on intact sinus venosus preparations. As the sinus venosus appears to be isopotential when arrested, we have made the simplifying assumption that the responses recorded from a point in such a syncytium can be modelled by treating the preparation as a small isopotential sheet of homogeneous cells. This does not mean that in reality every current, or channel set, is present in every individual sinus

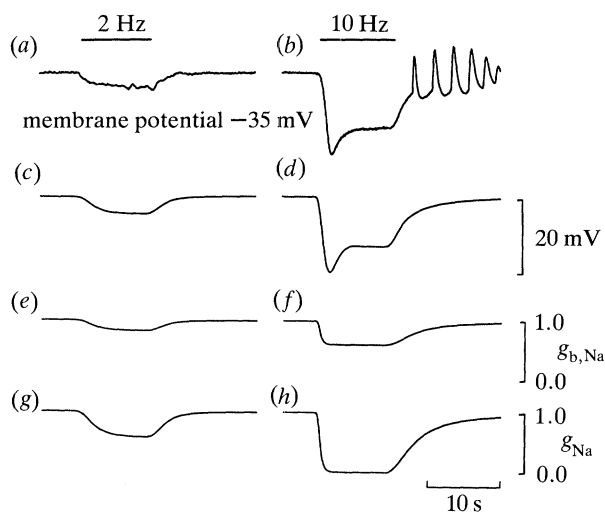


Figure 6. Effects of vagal stimulation on the membrane potential of arrested sinus venous cells. Traces (a) and (b) were recorded from a sinus venous preparation in which beating had been abolished by adding nicardipine, 1×10^{-5} M, to the perfusion fluid; the steady membrane potential was -35 mV. In (a) supramaximal bilateral vagal stimuli were applied for 10 s at a frequency of 2 Hz; in (b) the frequency of stimulation was 10 Hz. Both trains of stimuli produced hyperpolarizations but the response to the higher frequency of stimulation, although having a larger peak amplitude, was not sustained. Traces (c) and (d) show the simulations of these membrane potential changes which resulted from a suppression of the background sodium conductance, (e) and (f), along with a suppression of the voltage-dependent sodium conductance, (g) and (h). The voltage calibration bar refers to traces (a–d). The conductance calibration bars represent the conductance modulations applied to $g_{b,Na}$ and g_{Na} normalized about their control values. The time calibration bar refers to all records.

venous cell. To take an example, it may be that only a few cells contain TTX-sensitive channels and these cells in isolation may not generate pacemaking activity (see Brown *et al.* 1977). Yet when coupled into a syncytium, those cells would contribute an inward current during diastole. Thus our analysis should give a description of pacemaking activity in a functional syncytium; this may differ from the description derived more rigorously from a selected population of single cells (see, for example, Rassmusson *et al.* 1990).

(b) Simulation of inhibitory junction potentials recorded from arrested sinus venous cells

Single supramaximal stimuli applied to the vagi initiated inhibitory junction potentials, IJPs, with amplitudes of about 2 mV and durations of about 10 s (Hartzell 1979; Bywater *et al.* 1990). When the vagi were stimulated with trains of stimuli, the IJPs summed to give characteristic hyperpolarizations. With low-frequency stimulation, 1–2 Hz, a sustained hyperpolarization was recorded (figure 6a). With higher-frequency stimulation, 5–10 Hz, an initial rapid hyperpolarization was followed by a plateau phase more positive than the peak hyperpolarization

(figure 6b). Each of these potential changes was abolished by hyoscine (1×10^{-7} M) but persisted in the presence of Ba^{2+} (1 mM). IJPs also persisted in the presence of Cs^{+} (2–5 mM). During long trains of vagal stimuli, with Cs^{+} present, the membrane resistance of the arrested sinus cells increased by about 75%. This might suggest that vagally released ACh causes a hyperpolarization by closing existing membrane channels rather than opening additional channels (Bywater *et al.* 1990). IJPs were unaffected when the external concentration of chloride ions was reduced to one tenth of control by substituting sodium chloride either with equimolar sodium isethionate (three preparations) or with equimolar sodium methyl sulphate (three preparations).

Taken together these observations suggest that the responses to vagal stimulation do not result from an increase in potassium conductance involving channels that show inward rectification or from an increase in chloride conductance. Because the vagal responses could be recorded in the presence of very high concentrations of organic calcium antagonists and persisted in the presence of Cs^{+} , it is unlikely that the potential changes are initiated by a change in the activation potentials of hyperpolarization-activated Na/K channels or involve voltage-dependent Ca channels. The simplest explanation left is that vagal IJPs result from a decrease in sodium conductance, presumably $g_{b,Na}$.

Two features of the responses to trains of vagal stimuli require further comment. Firstly the characteristic relaxation which occurs during the hyperpolarizations produced by trains of high-frequency stimuli was abolished by adding Cs^{+} , 2–5 mM, to the physiological saline (figures 6b and 7b; see also Bywater *et al.* 1990). It has been suggested that the failure to sustain a steady hyperpolarization during a maintained vagal stimulus results from desensitization of muscarinic receptors (Jalife & Moe 1979). However, the finding that after the addition of Cs^{+} vagal stimulation causes a sustained hyperpolarization (figure 7b) suggests that the relaxation results from the activation of i_f . Thus in control solution, as the membrane hyperpolarizes under the influence of vagal stimulation, hyperpolarization activated Na/K channels open and the resulting inward current counteracts the hyperpolarization. As the relaxation first appears at membrane potentials of about -50 mV, the normal activation potential for hyperpolarization activated Na/K channels, it seems likely that vagally released ACh has little effect on these channels (c.f. DiFrancesco & Tromba 1988).

Secondly, when isolated segments of arrested pacemaker tissue were hyperpolarized by passing current through a second microelectrode, membrane potential oscillations were recorded: these were abolished by TTX (see figure 3). In contrast, membrane potential oscillations of this nature were never detected when the membrane was hyperpolarized by vagal stimulation delivered at 10 Hz (see figure 7b). On some occasions using lower frequencies of stimulation, small oscillations were detected; these were invariably abolished by increasing the frequency of stimulation. These observations raise the possibility that, as well as

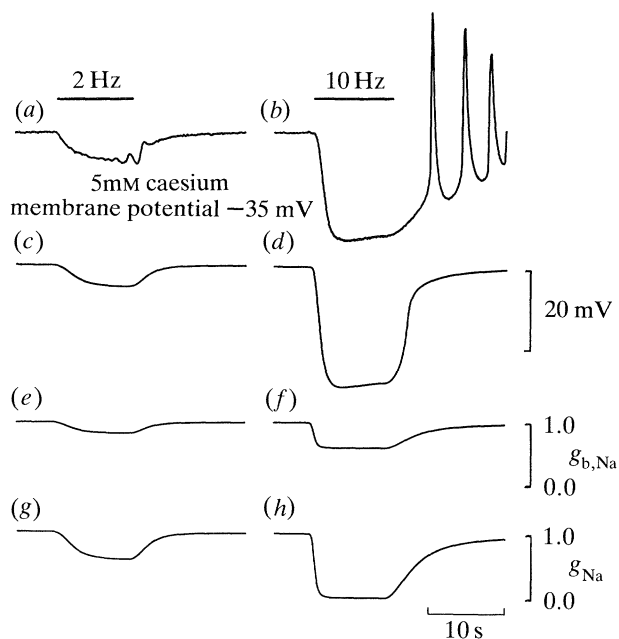


Figure 7. Effects of vagal stimulation on the membrane potential of arrested sinus venosus cells in the presence of Cs^+ . Traces (a) and (b) were recorded from the same preparation as shown in figure 6. Beating had been abolished by adding nicardpine, 1×10^{-5} M, to the perfusion fluid; the steady membrane potential was -35 mV. Hyperpolarization-activated Na/K channels were blocked by adding Cs^+ , 5 mM, to the physiological saline. In (a) supramaximal bilateral vagal stimuli were applied for 10 s at a frequency of 2 Hz; in (b) the frequency of stimulation was 10 Hz. Both trains of stimuli again produced hyperpolarizations. Now that produced by the higher frequency stimulation was larger in peak amplitude and was sustained. Traces (c) and (d) show the simulations of these membrane potential changes which resulted from a suppression of the background sodium conductance, (e) and (f), along with a suppression of the voltage-dependent sodium conductance, (g) and (h). The voltage calibration bar refers to traces (a–d). The conductance calibration bars represent the conductance modulations applied to $g_{b,\text{Na}}$ and g_{Na} normalized about their control values. The time calibration bar refers to all records.

reducing $g_{b,\text{Na}}$, vagally released ACh also prevents the activation of voltage-dependent Na channels (figures 6 and 7).

As a starting point, a description of the responses to vagal stimulation recorded from arrested pacemaker cells in the presence of Cs^+ was undertaken. The responses to single vagal stimuli could be readily modelled by assuming that they resulted solely from a reduction in $g_{b,\text{Na}}$ (for an example and justification see Bywater *et al.* (1990)). However, when this approach was used to describe the responses produced by trains of vagal stimuli the simulations did not match the experimental data. When $g_{b,\text{Na}}$ alone was reduced sufficiently to describe a large hyperpolarization, the simulations were interrupted by a series of membrane potential oscillations. In the simulations these resulted from the reactivation of voltage-dependent Na channels.

In the next attempt to simulate the timecourses of hyperpolarizations recorded during trains of vagal

stimuli, both $g_{b,\text{Na}}$ (figure 6*e,f*) and the conductance of voltage-dependent Na channels (figure 6*g,h*) were suppressed simultaneously. With this approach the timecourses of the responses to low- and high-frequency vagal stimulation could be described (figure 6*c–h*).

Subsequently the vagal responses recorded in control solution were emulated by including hyperpolarization-activated Na/K channels with their activation parameters being finely varied until the simulations matched data (figure 6*c,d*). Although the agreement between predictions and experimental data is acceptable both during the onset and during maintained vagal stimulation, the computational solutions do not provide an explanation for the series of regenerative potentials that followed large vagal hyperpolarizations. These regenerative potentials were simulated when it was assumed that during a vagal hyperpolarization some of the Ca channels showed voltage-dependent unblocking (see, for example, Nelson & Worley 1989): clearly this is not relevant to considerations of how vagal stimulation might slow and stop the generation of action potentials by normal pacemaker cells. In passing, it should be noted that when the magnitude of i_f was adjusted to give a good fit to data obtained from arrested preparations, after incorporating the same value into the beating pacemaker model, the suppression of this current gave about a 20% reduction in the calculated rate of generation of pacemaker action potentials (figure 4).

(c) Simulation of responses to vagal stimulation recorded from beating sinus venosus cells

When recordings were made from beating pacemaker cells, low-frequency trains of vagal stimuli (train duration 10 s, stimulation frequency 2 Hz) slowed the rate of action potential discharge. During slowing the peak diastolic potential increased by a few millivolts (Hutter & Trautwein 1955, 1956; Bywater *et al.* 1989). The most prominent change was a slowed rate of diastolic depolarization with the peak amplitude of action potentials and their rate of repolarization being little changed (figure 8*a*). The timecourse of pacemaker action potentials, recorded before vagal stimulation, was calculated as described previously (see figure 5). During the period of vagal stimulation both $g_{b,\text{Na}}$ and the conductance of the voltage-dependent Na channels were suppressed to a similar degree to that derived to fit data recorded from arrested preparations (see figure 6*e,g* and figure 7*e,g*). It can be seen that the rate of discharge of simulated pacemaker action potentials slowed (figure 8*b*) in much the same way as that recorded experimentally (figure 8*a*).

With higher frequencies of vagal stimulation (5–10 Hz), the discharge of action potentials stopped (figure 9*a*). At the start of the stimulation train, the maximum diastolic potential increased by a few millivolts, subsequently the membrane potential settled at a potential about 10 mV positive of the control maximum diastolic potential. The steady potential reached during complete vagal inhibition was about -55 mV (for further details see Bywater *et*

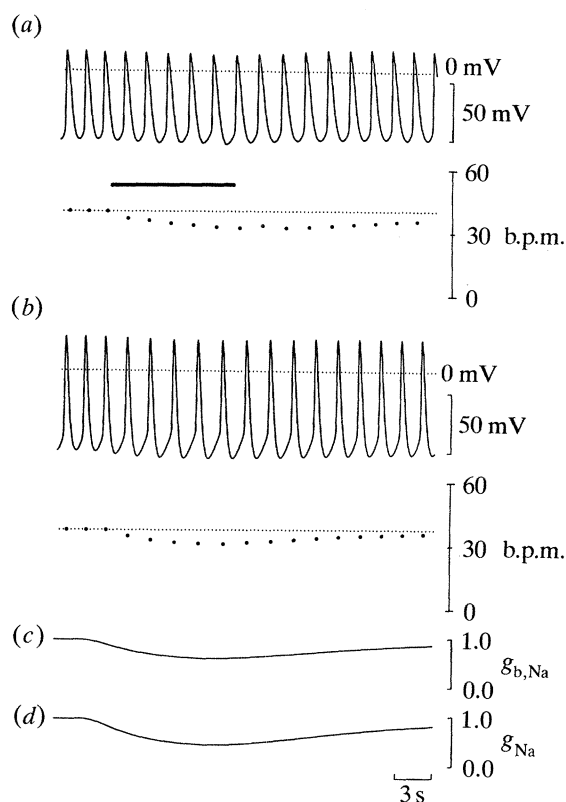


Figure 8. Effect of vagal stimulation on the discharge of action potentials recorded from toad sinus venosus. Trace (a), with associated tachograph, shows the membrane potential and rate change produced by bilateral vagal stimulation, 10 s at 2 Hz. Note there is a slight increase in peak diastolic potential and the rate of diastolic depolarization is slowed. In (b) a discharge of pacemaker action potentials, simulated as described in figure 5, is shown. During the trace, the background sodium conductance is reduced, trace (c), and the voltage-dependent sodium conductance is reduced, trace (d). The voltage calibration bars refer to traces (a) and (b). The conductance calibration bars represent the normalized conductance modulations applied to $g_{b,Na}$ and g_{Na} . The time calibration bar refers to all records.

al. 1989). After the period of vagal arrest, action potentials were again generated (figure 9a).

In the simulations, (figure 9b), it has been assumed that vagal slowing results from a suppression of $g_{b,Na}$ and a decrease in the conductance of voltage-dependent Na channels with similar conductance decreases to those shown in figure 7*f,h*, being applied. Again the simulations matched the experimental data.

(d) Effect of applying an inwardly rectifying potassium conductance to arrested and beating pacemaker cells

In most cardiac tissues added ACh activates muscarinic receptors which in turn open a set of K^+ selective ion channels. These channels are blocked by barium ions (Momose *et al.* 1984) and display inward rectification (Sakmann *et al.* 1983). The responses to vagal stimulation in both arrested and beating preparations were found to persist after adding barium ions to the physiological saline (Bywater *et al.* 1989, 1990).

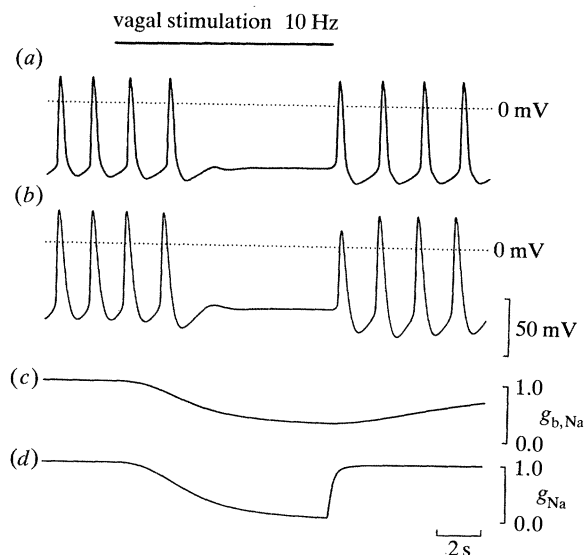


Figure 9. Effect of vagal stimulation on the discharge of action potentials recorded from toad sinus venosus. Trace (a) shows the membrane potential and rate change produced by bilateral vagal stimulation, 10 s at 10 Hz. Note that initially there is a slight increase in peak diastolic potential and the rate of diastolic depolarization is slowed, subsequently as beating stops, the membrane potential settles at a value positive of the peak diastolic potential. In trace (b) a discharge of pacemaker action potentials, simulated as described in figure 5, is shown. During the trace, the background sodium conductance is reduced dramatically, trace (c), and the voltage-dependent sodium conductance is reduced to zero, trace (d). The voltage calibration bar refers to traces (a) and (b). The conductance calibration bars represent the normalized conductance modulations applied to $g_{b,Na}$ and g_{Na} . The time calibration bar refers to all records.

To explore the possibility that neuronally released ACh opened a population of K channels that were resistant to barium blockade, the effects of neurally released ACh were modelled by applying an inwardly rectifying K conductance. The upper part of figure 10 shows the response of an arrested pacemaker cell to vagal stimulation and three simulations of this hyperpolarization produced by applying a three different increases in potassium conductance (figure 10*b*) sufficient to slow the generation of pacemaker action potentials. When these three different increases in potassium conductance were applied to the beating heart it can be seen that only the two more intense increases in potassium conductance caused arrest. It can also be seen that arrest was preceded by an increase in peak diastolic potential of some 15 mV and that the membrane potential settled near to the peak diastolic potential. A similar result to this has been given by Egan & Noble (1987). Experimental observations invariably show that during vagal arrest the membrane potential settles some 10–20 mV positive of the peak diastolic potential (Toda & West 1966; Bywater *et al.* 1989; Campbell *et al.* 1989). Hyperpolarizations like those predicted in the model have been recorded from beating pacemaker cells when ACh is applied (see Hartzell 1980; Ophof *et al.* 1987; Bywater *et al.* 1989; Campbell *et al.* 1989).

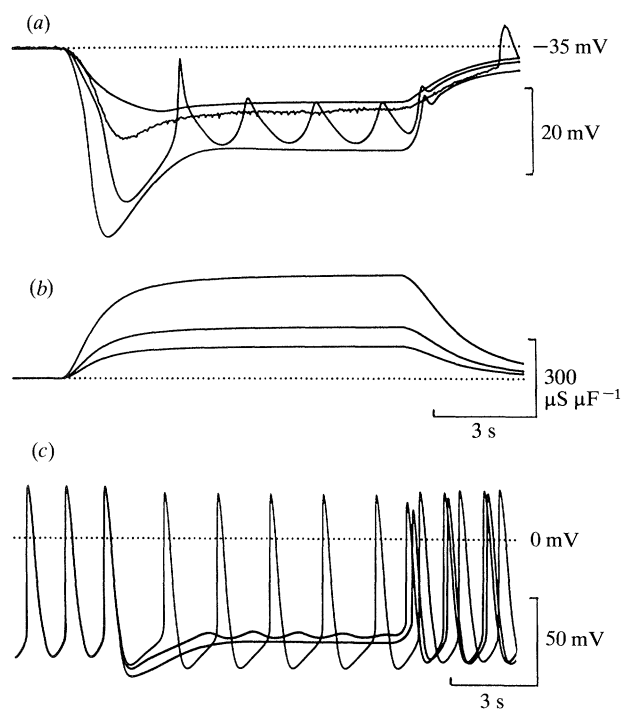


Figure 10. Attempts to describe the effects of vagal stimulation by assuming that neurally released acetylcholine activates an inwardly rectifying K^+ conductance. Trace (a) compares an experimental recording made from an arrested sinus venosus cell with three simulations in which an increase in K^+ conductance was applied. The magnitude of the conductance modulations is shown in (b). It can be seen that these three conductance modulations produced membrane potential changes that bracketed the experimental recording shown in (a). It is of interest to note that the intermediate conductance modulation produced a hyperpolarization that was interrupted by oscillations reminiscent of those recorded experimentally when segments of arrested sinus venosus preparation were hyperpolarized (see figure 3a). (c) When the three changes in K^+ conductance were applied to the beating heart simulation it can be seen that arrest only occurred if it was preceded by a large increase in peak diastolic potential. In practice, a stimulus like that presented in (a) invariably stopped the heart without a preceding large increase in peak diastolic potential. The upper time calibration bar refers to records (a) and (b); the lower time calibration bar refers to record (c).

Thus, although we could to some extent describe the changes in membrane potential recorded experimentally following vagal stimulation in an arrested preparation by a calculation involving an increase in potassium conductance, when an increase in potassium conductance was applied to the beating heart model the responses did not match those recorded experimentally (see figure 9).

4. DISCUSSION

(a) *Pacemaker potentials in toad sinus venosus cells*

In the first section of this paper the equations used by DiFrancesco & Noble (1985) were modified so that they gave an adequate description of pacemaking

activity in cells of the sinus venosus of the toad. Three inward currents were assumed to flow during diastole. These include contributions from two sets of voltage-dependent membrane channels. One set gave rise to a hyperpolarization-activated current, i_f or i_h (Yanagihara & Irisawa 1980; Brown 1982); the second set gave rise to an inward sodium current which flowed through TTX-sensitive channels. The third current was assumed to flow through a set of voltage-independent channels which give rise to a background sodium current.

In our description of pacemaking activity, an inward current during diastole is not provided by voltage-dependent Ca_T channels. However, there is evidence that such channels can contribute to pacemaking activity in some mammalian and amphibian pacemaker cells (Hagiwara *et al.* 1988; Bois & Lenfant 1991). We justify this omission by our observation that in the toad the rate of generation of pacemaker action potentials is not effected by adding nickel ions; these ions block Ca_T channels (Hagiwara *et al.* 1988). Nevertheless to describe pacemaking activity in toad sinus venosus cells it was necessary to make the threshold for activation of $i_{\text{Ca},f}$ some 25 mV more negative than that suggested by DiFrancesco & Noble (1985) but at a value close to that determined experimentally in amphibian pacemaker cells (Rasmusson *et al.* 1990).

An essential feature of our analysis is that for pacemaking activity to occur, delayed rectifier K channels show time-dependent deactivation. This idea is well supported by experimental observations by other workers (see Brown 1982) and will not be discussed further.

Thus we suggest that, in the toad, pacemaking occurs because, during the deactivation of delayed rectifier K channels, three separate inward currents flow during diastole. These currents are essentially carried by Na^+ ; in order of dominance the currents are provided by the background sodium conductance, by voltage-dependent Na channels and by hyperpolarization-activated Na/K channels. As the intensity of the outward K^+ current falls, the summed inward currents depolarize the membrane to threshold for inward calcium movement. Clearly, should the voltage-dependent Ca channels have been blocked pacemaking activity will also fail, a view again well justified by experimental observations.

(b) *Vagal inhibition of sinus venosus cells*

Vagal inhibition in toad and mammalian pacemaker cells is characterized by a reduction in the rate of diastolic depolarization until there is insufficient depolarization to initiate an action potential (Bywater *et al.* 1989; Campbell *et al.* 1989). When pacemaking is inhibited by adding an organic calcium antagonist to the physiological saline, vagal stimulation evokes membrane hyperpolarizations which are associated with an increase in the membrane resistance of sinus cells (Bywater *et al.* 1990).

Although it is generally held that neuronally released ACh activates muscarinic receptors which in

turn open inwardly rectifying K channels, few experimental observations support this view (see Shibata *et al.* 1985; Bywater *et al.* 1989; Campbell *et al.* 1989; Bywater *et al.* 1990). When we modelled the experimental data recorded from beating preparations as if it resulted from an increase in potassium conductance the computation did not agree with experimental observations (compare figures 9*a* and 10*c*). The conductance increase caused an increase in peak diastolic potential with the membrane potential settling near the control peak diastolic potential. A similar result has been given previously by Egan & Noble (1987). Finally it would be difficult to explain vagal inhibition in terms of opening additional membrane channels because, as has been pointed out, the membrane resistance of sinus venosus cells increases during stimulation of the vagus (Bywater *et al.* 1990).

A second way in which vagally released ACh might slow and stop the generation of pacemaker action potentials is to move the activation potential for hyperpolarization-activated Na/K channels to a more negative potential (DiFrancesco & Tromba 1987). It seems unlikely that vagally released ACh could act only in this way. The generation of pacemaker action potentials is only slowed, but not stopped, when these channels are blocked by Cs⁺ (DiFrancesco 1985). The effects of vagal stimulation in arrested preparations are not mimicked by Cs⁺ (Bywater *et al.* 1990). When recordings were made from arrested preparations, the experimental observations suggest that these channels were first activated at about -50 mV. This is about the normal potential at which hyperpolarization-activated Na/K channels start to open: an observation which implies that their activation potential remains unchanged during vagal stimulation (c.f. DiFrancesco & Tromba 1988). Nevertheless we cannot rule out the possibility that in beating preparations a part of the bradycardia results from an action of neuronally released ACh on these channels.

A third way in which vagally released ACh might slow the rate of generation of pacemaker action potentials is in some way to prevent the opening of voltage-dependent Ca channels (Shibata *et al.* 1985; Egan & Noble 1987). Should this be the case it is not clear how a suppression of voltage-dependent Ca channels would lead to a hyperpolarization in arrested preparations. At a membrane potential of -35 mV, in a solution containing a high concentration of organic calcium antagonist, one would expect all voltage-dependent Ca channels to be closed. Furthermore, in a simulation we found that, when the Ca conductance was reduced, the rate of generation of action potentials was little effected whereas the amplitudes of the action potentials was much reduced (see also Egan & Noble 1987).

We were able to describe our experimental observations when we reduced both the background sodium conductance and suppressed the voltage-dependent Na channels. With this approach a moderate decrease in $g_{b,Na}$ produced a hyperpolarization in an arrested preparation; a similar decrease slowed the rate of generation of action potentials (figure 8). A more intense decrease in $g_{b,Na}$ along with a suppression of

voltage-dependent Na channels which mimicked the hyperpolarization recorded from arrested preparations resulted in an increase in membrane resistance, $\approx 80\%$, similar to that observed experimentally. Similar changes in conductance stopped the generation of pacemaker action potentials. The membrane potential settled at a level positive of the peak diastolic potential but negative of the threshold for the initiation of action potentials (figure 9).

It is not clear whether the suppression of $g_{b,Na}$ and voltage-dependent Na current implies that both currents arise from subgroups of a common Na channel set which are in different conformational states. Furthermore, it is not clear how such a change in membrane Na⁺ conductance might occur. Vagal stimulation does not appear to involve the activation of muscarinic K channels, yet these channels are widely distributed over the surfaces of cardiac pacemaker cells. These two observations imply that neuronally released ACh must activate a set of specialized junctional receptors. Such junctional receptors presumably trigger the production of a second messenger substance which diffuses through the cell to reduce cell Na⁺ conductance. The more unlikely possibility is that the entire cell Na⁺ conductances are restricted to the neuroeffector junction, about 0.1% of the total cell surface area (Klemm *et al.* 1992), with these conductances, in some way, being directly coupled to the junctional receptors.

(c) Conclusions

The aim of these calculations was to explore the possibility that neuronally released ACh slowed the rate of generation of pacemaker action potentials by suppressing inward current flow during diastole. The first section aimed to provide a description of pacemaking activity in cells of the sinus venosus of the toad. To describe our experimental data it was necessary to allow inward current flow through three separate sets of ion channels during diastole. The subsequent analysis of data, which was obtained from experiments where responses to vagal stimulation were recorded, is consistent with the idea that the major effect of vagally released ACh is one of suppressing inward current flow during diastole. The calculations suggest that the inward movement of Na⁺ during diastole is suppressed (Bywater *et al.* 1990). The calculations lend little support to the views that vagally released ACh acts by increasing the conductance of pacemaker cells to potassium ions or by altering the properties of either voltage-dependent Ca channels or hyperpolarization-activated Na/K channels.

This project was supported by a research grant from the Australian N.H. and M.R.C. We thank them for their financial support.

REFERENCES

- Bois, P. & Lenfant, J. 1991 Evidence for two types of calcium currents in frog cardiac sinus venosus cells. *Pflügers Arch. Eur. J. Physiol.* **417**, 591–596.

- Bramich, N.J., Edwards, F.R. & Hirst, G.D.S. 1990 Sympathetic nerve stimulation and applied transmitters on the sinus venosus of the toad. *J. Physiol., Lond.* **429**, 349–375.
- Brown, H.F. 1982 Electrophysiology of the sinoatrial node. *Physiol. Rev.* **62**, 505–530.
- Brown, H.F., Giles, W. & Noble, S.J. 1977 Membrane currents underlying activity in frog sinus venosus. *J. Physiol., Lond.* **271**, 783–816.
- Bywater, R.A.R., Campbell, G., Edwards, F.R., Hirst, G.D.S. & O'Shea, J.E. 1989 The effects of vagal stimulation and applied acetylcholine on the sinus venosus of the toad. *J. Physiol., Lond.* **415**, 35–56.
- Bywater, R.A.R., Campbell, G., Edwards, F.R. & Hirst, G.D.S. 1990 Effects of vagal stimulation and applied acetylcholine on the arrested sinus venosus of the toad. *J. Physiol., Lond.* **425**, 1–27.
- Campbell, G., Edwards, F.R., Hirst, G.D.S. & O'Shea, J.E. 1989 Effects of vagal stimulation and applied acetylcholine on pacemaker potentials in the guinea-pig heart. *J. Physiol., Lond.* **415**, 57–68.
- Del Castillo, J. & Katz, B. 1955 Production of membrane potential changes in the frog's heart by inhibitory nerve impulses. *Nature, Lond.* **175**, 1035.
- Denyer, J.C. & Brown, H.F. 1990 Rabbit sino-atrial node cells: isolation and electrophysiological properties. *J. Physiol., Lond.* **428**, 405–424.
- DiFrancesco, D. 1985 The cardiac hyperpolarizing-activated current, i_f . Origins and developments. *Prog. Biophys. molec. Biol.* **46**, 163–193.
- DiFrancesco, D. & Noble, D. 1985 A model of cardiac electrical activity incorporating ionic pumps and concentration changes. *Phil. Trans. R. Soc. Lond. B* **307**, 353–398.
- DiFrancesco, D. & Noble, D. 1989 Current i_f and its contribution to cardiac pacemaking. In *Neuronal and cellular oscillators* (ed. J. W. Jacklet), pp 31–57. New York: Marcel Dekker.
- DiFrancesco, D. & Tromba, C. 1987 Acetylcholine inhibits activation of the hyperpolarizing-activated current, i_f . *Pflügers Arch. Eur. J. Physiol.* **410**, 139–142.
- DiFrancesco, D. & Tromba, C. 1988 Inhibition of the hyperpolarization-activated current (i_f) induced by acetylcholine in rabbit sino-atrial node myocytes. *J. Physiol., Lond.* **405**, 477–491.
- Egan, T.M. & Noble, S.J. 1987 Acetylcholine and the mammalian 'slow inward' current: a computer investigation. *Proc. R. Soc. Lond. B* **230**, 315–337.
- Giles, W. & Shibata, E. 1985 Voltage clamp of bull-frog cardiac pacemaker cells: a quantitative analysis of potassium currents. *J. Physiol., Lond.* **368**, 265–292.
- Hagiwara, N., Irisawa, H. & Kameyama, M. 1988 Contribution of two types of calcium currents to the pacemaker potentials of rabbit sino-atrial node. *J. Physiol., Lond.* **395**, 233–253.
- Hartzell, H.C. 1979 Adenosine receptors in frog sinus venosus: slow inhibitory potentials produced by adenine compounds and acetylcholine. *J. Physiol., Lond.* **293**, 23–49.
- Hartzell, H.C. 1980 Distribution of muscarinic acetylcholine receptors and presynaptic nerve terminals in amphibian heart. *J. Cell Biol.* **86**, 6–20.
- Hille, B. 1984 *Ionic channels of excitable membranes*. Sunderland, Massachusetts: Sinauer Associates.
- Hutter, O.F. & Trautwein, W. 1955 Effect of vagal stimulation on the sinus venosus of the frog's heart. *Nature, Lond.* **176**, 512–513.
- Hutter, O.F. & Trautwein, W. 1956 Vagal and sympathetic effects on the pacemaker fibres in the sinus venosus of the heart. *J. gen. Physiol.* **39**, 715–733.
- Jalife, J. & Moe, G.K. 1979 Phasic effects of vagal stimulation on pacemaker activity of the isolated sinus node of the young cat. *Circulation Res.* **45**, 595–607.
- Klemm, M.F., Hirst, G.D.S. & Campbell, G.D. 1992 Structure of autonomic neuroeffector junctions in the sinus venosus of the toad. *J. autonom. Nerv. Syst.* **39**, 139–150.
- Kreitner, D. 1975 Evidence for the existence of a rapid sodium channel in the membrane of rabbit sinoatrial cells. *J. molec. cell. Cardiol.* **7**, 655–662.
- Momose, Y., Giles, W. & Szabo, G. 1984 Acetylcholine-induced K^+ current in amphibian atrial cells. *Biophys. J.* **45**, 20–22.
- Nelson, M.T. & Worley, J.F. 1989 Dihydropyridine inhibition of single calcium channels and contraction in rabbit mesenteric artery depends on voltage. *J. Physiol., Lond.* **412**, 65–91.
- Noble, D. 1975 *The initiation of the heart beat*. Oxford: Clarendon Press.
- Noble, D. 1984 The surprising heart: a review of recent progress in cardiac electrophysiology. *J. Physiol., Lond.* **353**, 1–50.
- Noble, D., DiFrancesco, D. & Denyer, J. 1989 Ionic mechanisms in normal and abnormal cardiac pacemaker activity. In *Neuronal and cellular oscillators* (ed. J. W. Jacklet), pp 59–85. New York: Marcel Dekker.
- Noble, D. & Noble, S.J. 1984 A model of sino-atrial node electrical activity based on a modification of the DiFrancesco-Noble (1984) equations. *Proc. R. Soc. Lond. B* **222**, 295–304.
- Ophhof, T., Van Ginneken, A.C.G., Bouman, L.N. & Jongasma, H.F. 1987 The intrinsic cycle length in small pieces isolated from the rabbit sinoatrial node. *J. molec. cell. Cardiol.* **19**, 923–934.
- Rasmusson, R.L., Clark, J.W., Giles, W.R., Shibata, E.F. & Campbell, D.L. 1990 A mathematical model of a bullfrog cardiac pacemaker cell. *Am. J. Physiol.* **259**, H352–H369.
- Sakmann, B., Noma, A. & Trautwein, W. 1983 Acetylcholine activation of single muscarinic K^+ channels in isolated pacemaker cells of the mammalian heart. *Nature, Lond.* **303**, 250–253.
- Shibata, E.F. & Giles, W. 1985 Ionic currents that generate the spontaneous diastolic depolarization in individual cardiac pacemaker cells. *Proc. natn. Acad. Sci. U.S.A.* **82**, 7796–7800.
- Shibata, E.F., Giles, W. & Pollack, G.H. 1985 Threshold effects of acetylcholine on primary pacemaker cells of the rabbit sino-atrial node. *Proc. R. Soc. Lond. B* **223**, 355–378.
- Toda, N. & West, T.C. 1966 Changes in sinoatrial potentials on vagal stimulation of the isolated rabbit atrium. *Nature, Lond.* **205**, 808–809.
- Yanagihara, K. & Irisawa, H. 1980 Inward current activated during hyperpolarization in rabbit sinoatrial node cell. *Pflügers Arch. Eur. J. Physiol.* **385**, 11–19.

Submitted by D. Noble; received 15 October 1992; accepted 5 January 1993